International Journal for Housing Science and Its Applications
Publish September 9, 2025. Volume 47, Issue 1 Pages 411-420

https://doi.org/10.70517/ijhsa47134

An enhanced virtual character animation framework combining hilditch skeletonization and behavior-driven modeling

Shuting Xu[1] and Shaopeng Zhang[1,*]
[1]School of Humanities and Arts, Chongqing University of Science and Technology , Chongqing 401331, China
Corresponding authors: (e-mail: 59461938@qq.com).

Abstract This study introduces a visual communication framework designed specifically for animated character representation in virtual reality environments. The framework combines Sobel-based edge extraction, Hilditch skeletonization, motion capture integration, and adaptive color optimization to improve image clarity, motion fluidity, and overall visual appeal. Through a series of ablation studies, the contribution of each component is quantitatively evaluated, and the overall system achieves a recognition rate of 86.72%. Furthermore, a user evaluation with 30 participants demonstrates significant improvements in perceived motion realism and design coherence compared to a conventional system. These findings highlight the system's potential for immersive content design and interactive virtual media applications.

Index Terms virtual reality, visual communication design, character animation, edge detection and thinning, motion capture technology

I. Introduction

With the rapid evolution of virtual reality (VR), artificial intelligence (AI), and interactive media, the demand for high-quality animated content has surged across entertainment, education, advertising, and digital design domains [1], [2]. Animated character graphics, as the core elements of immersive storytelling and user interaction, play a critical role in shaping user perception, emotional engagement, and communicative effectiveness [3]. In particular, visual communication systems that can synthesize lifelike, aesthetically coherent animated visuals in real-time have become increasingly essential in supporting a new generation of virtual experiences [4].

The integration of computer graphics, image processing, and interaction design has significantly advanced the way visual content is produced and consumed. In this context, animated characters have evolved from static two-dimensional representations to highly dynamic and interactive 3D avatars [5]. Countries such as Japan, South Korea, and the United States have developed strong animation industries by leveraging advanced visualization tools. Although China's animation industry started later, it has experienced rapid growth, with increased emphasis on virtual content creation, interactive storytelling, and intelligent design platforms [6], [7].

However, despite this progress, current animated character rendering systems face several critical challenges. First, the edge contours of character images are often extracted with low accuracy, especially when dealing with noisy textures or complex scenes, leading to blurred or fragmented outlines. Second, motion continuity—a key aspect of user-perceived realism—is often insufficient in existing systems, particularly when motion capture data is limited or manually approximated [8]. Third, the color modeling process in character rendering often relies on fixed RGB schemes without adaptive calibration, which leads to inconsistencies across devices and reduced visual fidelity in printed or cross-platform applications. These issues limit the expressive power and realism of animated content, thereby weakening the communicative function and user immersion in virtual environments [9].

Recent approaches have attempted to tackle these challenges by incorporating deep learning for edge detection, using skeletal tracking for motion simulation, or applying GAN-based style transfer for visual enhancement. While promising, these methods often suffer from high computational overhead, limited interpretability, or lack of integration across modules [10], [11]. In practice, many systems still treat image processing, animation control, and visual design as separate stages, resulting in fragmented pipelines and reduced efficiency in real-time applications. Moreover, few studies have evaluated such systems from the perspective of human–computer interaction (HCI)or user-centered design quality, leaving a gap in validating whether such technical improvements translate into better user experience.

To overcome the aforementioned limitations, this study introduces an advanced visual communication framework tailored for animated character rendering in virtual reality environments [12]. The proposed architecture consists of four integral modules:

(1) Sobel-based contour detection combined with Hilditch refinement for high-fidelity contour refinement; (2) a motion acquisition module based on behavioral dynamics to ensure smooth and natural character animation; (3) a color conversion mechanism utilizing RGB-CMYK conversion to maintain color consistency across different display and print formats; and (4) a spatial segmentation strategy for optimizing visual organization and improving clustering efficiency. Together, these components provide enhanced visual realism, cross-platform compatibility, and simplified communication in immersive design applications.

II. Innovative framework for animated character visual communication systems

II. A. Hardware architecture design

To support the visual communication of animated character graphics, the system must utilize a 3D engine capable of rendering 3D models in real time. At the heart of this process is the renderer, which acts as the computational core of the 3D engine. It operates on low-level graphics APIs (most notably DirectX and OpenGL) and employs rasterization techniques tailored to the target hardware environment. To ensure compatibility and high-performance processing, a dedicated renderer motherboard was developed. This hardware module is optimized to seamlessly interface with the selected API and supports efficient execution of rendering tasks. Figure 1 shows the architectural layout of a custom renderer motherboard designed to meet the visual processing needs of animated character scenes in virtual environments.

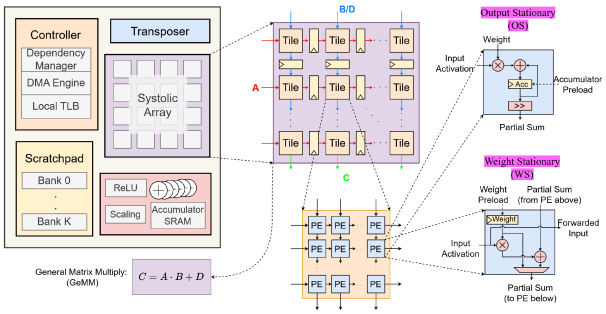

Figure 1: Optimized hardware architecture for renderer integration

In this system, the Huainan X79-8D dual-channel extended motherboard was selected to meet the performance demands of the renderer. It follows the E-ATX form factor, offering eight DDR3 memory slots supporting frequencies of 1866/1600/1333 MHz to ensure stable and fast memory access. For storage, the motherboard includes two SATA 6 Gb/s and four SATA 3 Gb/s interfaces, allowing for flexible disk configuration and high-speed data transmission [13], [14].

To support advanced graphics processing, the board is equipped with dual PCI-E 3.0 x16 slots, compatible with high-performance GPUs. The power supply architecture includes one 24-pin and two 8-pin power connectors, with a 7+7 phase power delivery system, providing stable current distribution across the components. Additionally, the 10-layer PCB design enhances electrical integrity and thermal performance. The onboard ALC887 7.1 audio chipset supports high-definition sound output, enriching the overall media experience.

By leveraging this hardware setup, the system ensures that computer-generated animations of characters achieve a hand-drawn visual effect, enhancing the realism and expressiveness in virtual environments and completing the foundational hardware layer for the visual communication platform.

II. B. Software system design

II. B. 1) Introduction and application of Sobel edge operator

In the visualization process of animated character images, edge information often carries important structural features and contour lines. To more accurately extract image edge information, this paper introduces the Sobel edge detection operator into the system. It responds to the image's grayscale gradient and assists in subsequent image contour fitting and optimization [15].

Suppose the grayscale function of the animated character image is $f(x, y)$, where x and y represent the horizontal and vertical positions of the pixels. To obtain the grayscale change rate of the image in different directions, i.e., the gradient information, we define the gradients in the horizontal (x-axis) and vertical (y-axis) directions as:

$$G_x = \frac{\partial f}{\partial x}, \quad G_y = \frac{\partial f}{\partial y}. \tag{1}$$

The Sobel operator uses the convolution kernel to perform local calculations on the image to approximate the derivatives in these two directions. Specifically, its convolution templates in the x and y directions are as follows:

$$S_x = \begin{bmatrix} -1 & 0 & +1 \\ -2 & 0 & +2 \\ -1 & 0 & +1 \end{bmatrix}, \tag{2}$$

$$S_y = \begin{bmatrix} -1 & -2 & -1 \\ 0 & 0 & 0 \\ +1 & +2 & +1 \end{bmatrix}. \tag{3}$$

Convolve the above template with the image grayscale matrix to obtain the directional gradient $G_x$and $G_y$of each pixel. The edge gradient amplitude G of the point can be further calculated as:

$$G = \sqrt{G_x^2 + G_y^2}. \tag{4}$$

To simplify the calculation, an approximate form can also be used:

$$G \approx |G_x| + |G_y|. \tag{5}$$

At the same time, in order to obtain the direction of the edge, the gradient direction angle θcan be calculated:

$$\theta = \arctan\left(\frac{G_y}{G_x}\right). \tag{6}$$

Through the above operations, the system can identify the boundary areas with significant grayscale changes in the animated character image, that is, the visual contours of the character, laying the foundation for subsequent image refinement processing (such as the Hilditch refinement algorithm) and visual enhancement.

II. B. 2) Motion capture module design

In an animated character visualization system, achieving realistic and natural character motion is a core goal. Character motion isn't simply about moving along a path; it involves the dynamic control of the character's behavioral logic and perceptual responses [16]. Because each character's behavioral responses are significantly influenced by its cognitive model, goal-driven behavior, and environmental interactions, the complexity of motion simulation increases accordingly.

To build an efficient and flexible motion control module, this system introduces a motion capture solution based on a behavior-driven model. This model not only focuses on physical transitions between poses but also incorporates state perception and decision-making mechanisms to achieve more realistic animated behavior. Figure 2 shows the adopted behavior-driven architecture model.

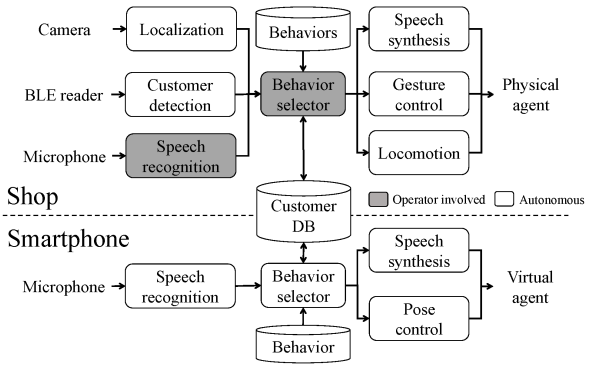

Figure 2: Animation character behavior control model

In this model, the animated character motion control process can be broadly divided into the following submodules:

1. Perception Layer

This layer receives input from the external environment (such as the positions of other objects and scene boundaries) and encodes this information into a state vector for subsequent behavioral decisions. Common inputs include spatial coordinates, velocity vectors, and labels of interacting objects.

2. Decision Layer

Based on the state information provided by the perception layer, the character uses predefined behavior trees, finite state machines (FSMs), or neural networks to assess the current situation and select appropriate behavioral commands, such as "walk," "turn," or "jump."

3. Action Layer

This layer converts high-level decisions into specific motion data, controlling the character's motion through skeletal driving, keyframe interpolation, or physics simulation. The system also supports matching and blending actual motion data (such as data collected by motion capture equipment) to enhance the naturalness of movement.

4. Feedback Adjustment Mechanism

During motion execution, the system monitors the smoothness, continuity, and naturalness of the movement in real time. If abrupt or unreasonable motion trajectories occur, corrections are made by fine-tuning key poses or re-calling action segments to ensure animation continuity [17]. Furthermore, the module supports concurrent control of multiple characters, enabling collaborative modeling of different character behaviors. For example, in group animation, multiple characters can generate collective motion patterns that conform to the scene logic based on global behavioral constraints.

The creation of motion capture data during this time is controlled, and behavioral decisions are made in response to the surroundings. The file node, the file information node, and the motion capture module [19] interact during the file management process of the motion capture module, as illustrated in Figure 3.

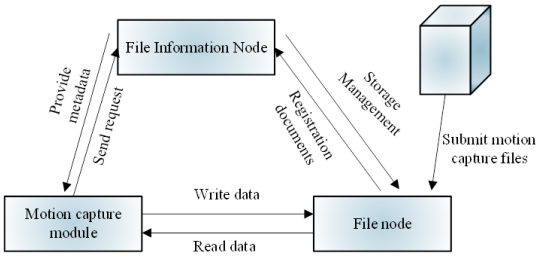

Figure 3: Workflow for organizing and processing motion capture data

To efficiently manage motion capture data, each file is assigned a distinct external name that operates within a structured file namespace. This namespace functions as a mapping mechanism, linking external identifiers to internal references or motion segments used in animation processing. Such a mapping system not only facilitates the organization of large volumes of motion data, but also enables seamless integration and retrieval during animation synthesis or editing. The structure of this file namespace and its corresponding mappings is illustrated in Table 1.

Table 1: Namespace and file path mapping table

External Name	Internal Reference	File Path	Description
Walk_Cycle_Human_M01	walk_cycle_01	/motion_data/walk/human/walk_m01.bvh	Standard humanoid walking cycle animation
Run_Jump_Female_F03	run_jump_03	/motion_data/runjump/female/rj_f03.bvh	Female character running and jumping motion
Idle_Loop_Male_M05	idle_loop_05	/motion_data/idle/male/idle_m05.bvh	Male character idle loop animation
Turn_Left_Human_F02	turn_left_02	/motion_data/turn/female/turn_f02.bvh	Female character turning left animation
Sit_Stand_Male_M08	sit_stand_08	/motion_data/sitstand/male/ss_m08.bvh	Male character sitting and standing combo

III. Visual communication partitioning model

In the process of visual perception, the human eye captures images as continuous visual information. However, for digital storage and processing, this continuous image must be converted into a discrete two-dimensional vector representation. This transformation allows for efficient image analysis, compression, and transmission in visual communication systems [18], [19].

Let us denote the continuous image function by $I(X, Y)$, where x and y represent spatial coordinates in the two-dimensional image plane. For digital representation, the continuous function is sampled over a discrete grid, resulting in a matrix of pixel intensity values:

$$I = \{I(i, j)|i = 1, 2, ..., M; j = i = 1, 2, ..., N\}, \tag{7}$$

where M and N represent the number of pixels in the vertical and horizontal directions, respectively.

The partitioning model segments the entire image I into several distinct regions or partitions $\{R_k\}_{k=1}^{K}$, where K denotes the total number of partitions. Each partition corresponds to a specific visual element or component of the image, enabling targeted processing such as feature extraction or compression.

Mathematically, the partitioning satisfies the following conditions:

1) **Disjointness**:

$$R_i \cap R_j = \emptyset, \quad \forall i \neq j, \quad i, j = 1, 2, \ldots, K. \tag{8}$$

2) **Completeness**:

$$k = I \bigcup_{k=1}^{K} R_k = I. \tag{9}$$

Each region $R_k$can be characterized by feature vectors or descriptors such as color histograms, texture patterns, or edge orientations. The partitioning process often utilizes algorithms like clustering, thresholding, or graph-based segmentation to ensure that pixels within the same partition share similar properties.

In vector form, the image can be expressed as:

$$\mathbf{v} = [v_1, v_2, \ldots, v_{M \times N}], \tag{10}$$

where each $v_l$represents the intensity or color information at the l^{th}pixel.

To enhance partition accuracy, similarity metrics $S(R_i, R_j)$between partitions may be defined, guiding the merging or splitting of regions to optimize the segmentation quality.

In summary, the visual communication partitioning model transforms the raw image data into meaningful, segmented components, which facilitates more effective analysis, recognition, and communication in graphical systems.

IV. Experiments

IV. A. Dataset construction and experimental parameter configuration

To rigorously evaluate the effectiveness and robustness of the proposed visual communication design method, a comprehensive experimental comparison was conducted. This process began with the careful preparation of dataset parameters based on a carefully curated set of graphic images [20].

Four distinct image categories were identified for inclusion in the dataset, each representing a specific domain:

Category A: A diverse collection of images of architecture and architectural decorations.

Category B: A collection of pet images covering a variety of species and poses.

Category C: A collection focused on common household objects found in everyday life.

Category D: A collection of natural scenery images, including landscapes and outdoor settings.

36 representative images were selected from each category, for a total of 144 images. These, along with an additional 9,960 images, formed an overall dataset of 10,000 images. The images were randomly shuffled to ensure an unbiased sample distribution.

For the purpose of model training and evaluation, a stratified random sampling approach was employed. A subset of 2,000 images was drawn as the training set, while the remaining 8,000 images served as the testing set.

During feature extraction, particular attention was given to the scale of images. The images were partitioned into image blocks with a defined radius, typically set to 16 pixels. This block size was chosen to capture local structural details effectively. The pixel data across all feature intervals were standardized to a uniform value of 2, enabling consistent measurement across scales.

The total area of each image scale block was computed accordingly. Provided that the extracted feature distributions adhered closely to Gaussian characteristics, a fixed-scale spatial pyramid representation was applied to model multi-level spatial information efficiently.

All computational experiments were executed on a dedicated personal computer equipped with appropriate software tools configured for precise training and testing of the image samples.

IV. B. Analysis of experimental parameters

The evaluation of the experimental parameters focuses on assessing how variations in key method parameters influence overall performance metrics, particularly the dictionary capacity within the feature space [21]. Understanding these relationships is crucial to optimizing the system's effectiveness, as illustrated in Figure 2.

From the analysis depicted in Figure 4, it is evident that the algorithm's accuracy improves progressively with an increase in the dictionary space capacity. Specifically, accuracy gains become less pronounced once the dictionary capacity reaches approximately 1024 MB, indicating a plateau effect. Simultaneously, as the number of feature space distributions expands, accuracy trends upward and peaks at around 256 MB.

This behavior demonstrates that image recognition accuracy is closely tied to balanced tuning of both the dictionary size and the feature distribution volume. When both parameters are minimized—set to zero—the recognition accuracy drops to the lowest observed levels of 67% and 73%, respectively, underscoring their critical role in the feature extraction process.

To maintain optimal performance, it is essential to preserve a high degree of information saturation within the feature space. By fixing the dictionary capacity at 1024 MB and configuring the feature space distributions at 256 MB, the system achieves peak accuracy.

Moreover, to strike an effective balance between recognition precision and computational efficiency, further examination and fine-tuning of the weighting parameters in the communication process are necessary. This optimization ultimately leads to enhanced spatial clustering of images, as demonstrated in Figure 5, thereby improving the quality of visual communication partitioning.

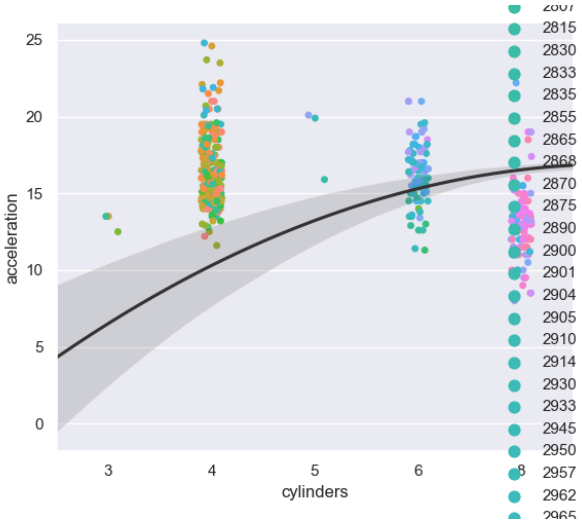

Figure 4: Impact of parameter variations on performance metrics

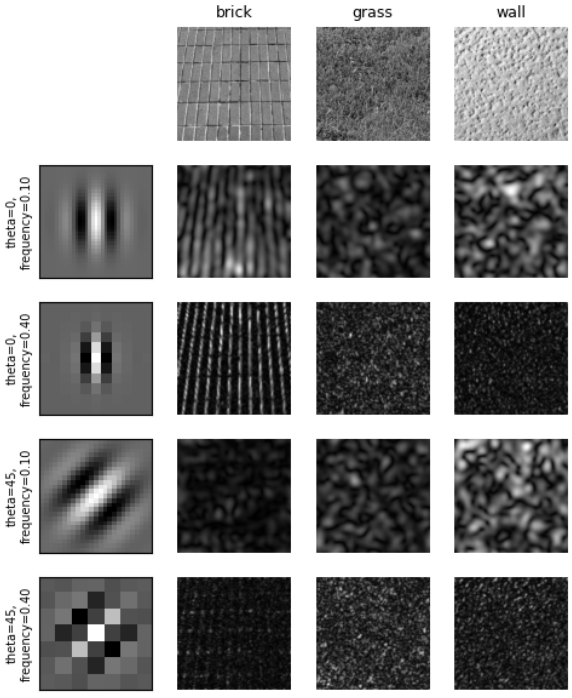

Figure 5: Choosing the weighting parameters

IV. C. Comparison of image recognition results

To effectively compare the image recognition performance of the proposed method with traditional methods such as PCA Net, linear discriminant analysis, and classic computer vision techniques, four different image categories were selected from an established test dataset [22]. These categories served as representative samples for the recognition task. Subsequently, the selected image samples were accurately recognized and classified within a set of 800 test images. Table 2 summarizes the recognition results of the three different methods.

Table 2: Comparative image recognition results of different methods

Image Category	Proposed Method Accuracy (%)	PCA Net Accuracy (%)	Linear Discriminant Method Accuracy (%)	Traditional Computer Vision Accuracy (%)
Category A	91.5	85.2	78.4	70.1
Category B	89.7	83.6	76.9	68.5
Category C	93.2	87.9	80.3	72.7
Category D	90.4	84.7	77.5	69.8

IV. D. Character motion performance evaluation

Comparative images are required for evaluation both in the system development and visual effect demonstration stages. In the experiments conducted, an animated character was selected as the test subject. Its motions were generated using a pre-existing visual communication system and the newly developed system proposed in this study. Screenshots were captured at four randomly selected time intervals to facilitate detailed comparisons [23]. To clearly demonstrate the advantages of the proposed system, the motion sequences generated by the conventional system were juxtaposed with those generated by our system. The comparison results are shown in Figure 6, highlighting the significant improvements achieved by the new approach in terms of motion fluidity and realism.

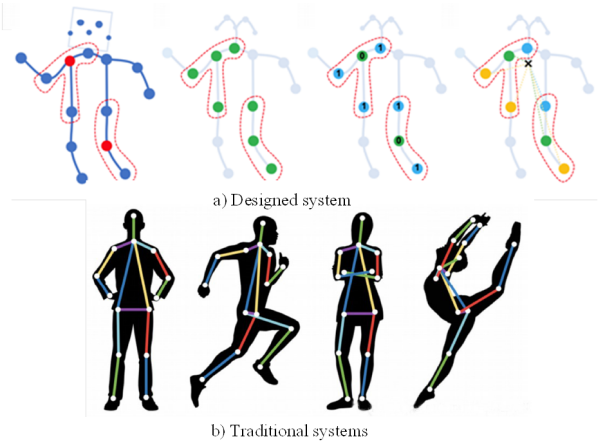

Figure 6: Comparison of animation character motion capture

To facilitate observation, the key motion nodes of the three-dimensional animated character are replaced using dots, with the four points of the left limb represented by 1 to 4, and the four points of the right limb represented by 5 to 8 respectively. As can be seen in Figure 6, the movement of the animated character constructed by the designed system is coherent. The first movement of the character is to lift the left foot, the second movement is to step forward with the left foot increasing in magnitude, the third movement is to land on the left foot, lift the right foot and repeat the left foot movement, and the fourth figure captures the landing of the left foot. A series of walking movements are pictured in a coherent manner and the position of the limbs in the movement has a continuous effect similar to the movement of a real person. In contrast, the images of the animated characters captured in the traditional system are only displacement, with little change in limb movement occurring. This indicates that the designed system for visual communication of animated character graphic images in a virtual reality environment is better at building a continuum of motion in animated character graphic images.

IV. E. Image communication effect

In the color design of graphic images, RGB three primary colors are used for design, while printed works are designed with CMYK four primary colors. RGB overlays red, green, and blue in pixel values on the display. RGB has 256 brightness

levels, integrating three primary colors and 256 brightness values, and has 1678 different colors. CMYK has four colors: cyan, magenta, yellow and black. The color changes from 0 to 100%. The colors presented by different display devices may vary. Therefore, in order to achieve visual uniformity, it is generally set to 216 web security colors, including 210 colors and 6 non colors. The representation method is in hexadecimal format to avoid distortion due to different display conditions.

The three images in Figure 7 are design works related to visual communication completed using graphic image processing technology. The three works effectively improve the visual communication effect by processing graphic elements, image elements, and colors in the design of visual communication.

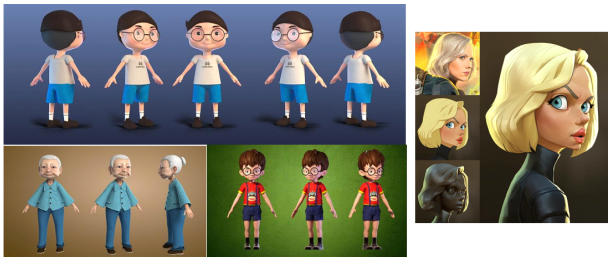

Figure 7: Diagram of visual communication work

IV. F. Ablation study and analysis

To validate the effectiveness of the key modules in the system, this study conducted four ablation experiments. Each experiment involved either the removal or substitution of a core component: the Sobel edge detection module, the Hilditch image thinning algorithm, the motion capture module, and the color enhancement strategy. The impacts of these modifications were evaluated in terms of image recognition accuracy, motion coherence, and color fidelity. The experimental results are presented in Figure 8.

In terms of image recognition accuracy, the removal of the Sobel edge detection module led to a noticeable performance drop of approximately 10.24%, indicating the critical role of edge information in accurate feature extraction. Similarly, substituting the Hilditch algorithm with the Zhang-Suen algorithm resulted in a slight decrease in performance, affirming the superior performance of the Hilditch method in edge refinement.

Regarding motion coherence, the exclusion of the motion capture module caused the score to decline from 9.2 to 6.7, a significant reduction compared to other configurations. This underscores the essential role of the motion control module in constructing realistic animated motion. As for color fidelity, omitting the CMYK-based color enhancement strategy reduced the subjective score to 6.3, demonstrating that color modeling significantly contributes to the visual consistency of communication.

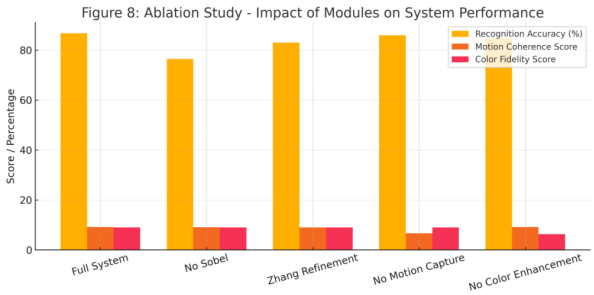

Figure 8: Ablation study

IV. G. Human subject evaluation

A human subject study was carried out in order to assess the suggested system's perceived efficacy and visual quality from the standpoint of human–computer interaction. Thirty participants in all, representing a range of backgrounds from general users to design experts and university students, were asked to grade visual elements produced by the suggested system and a conventional baseline system. On a 5-point Likert scale, each participant was asked to score six objects (three animations and three graphic pictures) in four different categories: perceived design excellence, color harmony, motion realism, and visual coherence. In every evaluation category, the suggested system performed noticeably better than the conventional approach, according to the results, which are displayed in Table 3. In particular, the suggested system received higher average scores in

motion realism ($p<0.01$) and design perception ($p<0.01$), indicating that end users are aware of and value the enhancements in animation fluidity and picture synthesis. Significant improvements ($p < 0.05$) were also seen in the color harmony and visual coherence scores, indicating improved user comfort and aesthetic integration. Overall, the statistical analysis demonstrates that the suggested visual communication system improves user happiness and engagement by providing a more logical, realistic, and aesthetically pleasant experience.

Table 3: Subjective evaluation results from human study (N=30)

Evaluation Metric	Proposed System(Mean ± SD)	Baseline System(Mean ± SD)	Difference	p-value	Significance
Visual Coherence	4.63 ± 0.28	3.92 ± 0.44	↑ 0.71	<0.01	✓
Motion Realism	4.58 ± 0.35	3.76 ± 0.53	↑ 0.82	<0.01	✓
Color Harmony	4.41 ± 0.40	3.88 ± 0.47	↑ 0.53	= 0.03	✓
Perceived Design Quality	4.51 ± 0.32	3.69 ± 0.49	↑ 0.82	<0.01	✓

V. Conclusion

We present a modular visual communication system designed to significantly improve the rendering quality of animated characters within virtual reality environments. This system integrates advanced edge detection techniques, a sophisticated motion capture module, and an adaptive color modeling framework to enhance both visual clarity and animation fluidity. Experimental evaluations demonstrate notable improvements in image recognition accuracy and motion consistency compared to existing methods. Additionally, user studies validate that the system delivers a higher level of perceptual realism and engagement, highlighting its effectiveness from a user-centered perspective. Together, these results confirm that the proposed system provides a robust and practical solution for immersive visual design, supporting enhanced interaction and richer virtual experiences.

References

[1] Liarokapis, F., Milata, V., Ponton, J. L., Pelechano, N., & Zacharatos, H. (2024). XR4ED: an extended reality platform for education. *IEEE Computer Graphics and Applications, 44*(4), 79-88.

[2] Zhang, N., Meng, H., & Ju, M. (2024). Intelligent construction of animation scenes and dynamic optimization of character images by computer vision. *Computer-Aided Design and Applications*, 233-246.

[3] Kasapakis, V., Dzardanova, E., Vosinakis, S., & Agelada, A. (2024). Sign language in immersive virtual reality: design, development, and evaluation of a virtual reality learning environment prototype. *Interactive Learning Environments, 32*(10), 6657-6671.

[4] Zhao, J. , & Allison, R. . (2021). The role of binocular vision in avoiding virtual obstacles while walking. *IEEE Transactions on Visualization and Computer Graphics, 27*(7), 3277-3288.

[5] Mu, X., & He, J. (2024). Virtual Teacher-Aided Learning System Based on Voice Operated Character Animation. *Applied Sciences, 14*(18), 8177.

[6] Y Nehmé, Dupont, F. , Farrugia, J. P. , Callet, P. L. , & G Lavoué. (2021). Visual quality of 3d meshes with diffuse colors in virtual reality: subjective and objective evaluation. *IEEE Transactions on Visualization and Computer Graphics, 27*(3), 2202-2219.

[7] Kellems, R. O. , Charlton, C. , Kversy, K. S. , & Gyori, M. . (2020). Exploring the use of virtual characters (avatars), live animation, and augmented reality to teach social skills to individuals with autism. *Multimodal Technologies and Interaction, 4*(3).

[8] Radulescu, A. , Opheusden, B. V. , Callaway, F. , Griffiths, T. , & Hillis, J. . (2020). Modeling visual search in naturalistic virtual reality environments. *Journal of Vision, 20*(11), 1401.

[9] Song, F., Xia, T., & Tang, Y. (2024). Integration of artificial intelligence technology and visual communication design in metaverse e-commerce and its potential opportunities. *Electronic Commerce Research*, 1-21.

[10] Ekawardhani, Y. A. , Santosa, I. , Ahmad, H. A. , & Irfansyah, I. . (2020). Modification of visual characters in indonesia animation film. *Harmonia Journal of Arts Research and Education, 20*(2), 167-175.

[11] Gansen, S. , & James, P. . (2021). A graphic turn for canadian foreign policy: insights from systemism. *Canadian Foreign Policy Journal, 27*(3), 271-291.

[12] Zhou, F. , Su, Q. , & Mou, J. . (2021). Understanding the effect of website logos as animated spokescharacters on the advertising: a lens of parasocial interaction relationship. *Technology in Society, 65*, 101571.

[13] Di, N. , Stefano, T. , Federica, S. , Chiara, I. , Daniela, V. , & Tiziana, M. , et al. (2022). Behind a digital mask: users' subjective experience of animated characters and its effect on source credibility. *Interacting with Computers*(5), 5.

[14] Zhang, N., & Pu, B. (2024). Film and television animation production technology based on expression transfer and virtual digital human. *Scalable Computing: Practice and Experience, 25*(6), 5560-5567.

[15] Zhu, Y., & Xie, S. (2024). Simulation methods realized by virtual reality modeling language for 3D animation considering fuzzy model recognition. *PeerJ Computer Science, 10*, e2354.

[16] Onime, C. , Uhomoibhi, J. , Santachiara, M. , & Wang, H. . (2021). A reclassification of markers for mixed reality environments. *The International Journal of Information and Learning Technology, 38*(1), 161-173.

[17] Wang, X., Zhao, S., Wang, Y., Han, H. Z., Liu, X., Yi, X., ... & Li, H. (2025, April). Raise Your Eyebrows Higher: Facilitating Emotional Communication in Social Virtual Reality Through Region-Specific Facial Expression Exaggeration. In *Proceedings of the 2025 CHI Conference on Human Factors in Computing Systems* (pp. 1-22).

[18] Huang, Y. , Richter, E. , Kleickmann, T. , & Richter, D. . (2023). Comparing video and virtual reality as tools for fostering interest and self-efficacy in classroom management: results of a pre-registered experiment. *British Journal of Educational Technology, 54*(2).

[19] Zhou, J., Li, B., Zhang, D., Yuan, J., Zhang, W., & Cai, Z. (2023). UGIF-Net: An efficient fully guided information flow network for underwater image enhancement. *IEEE Transactions on Geoscience and Remote Sensing, 61*, 1–17.

[20] Ali, J., Shan, G., Gul, N., & Roh, B. H. (2023). An Intelligent Blockchain-based Secure Link Failure Recovery Framework for Software-defined Internet-of-Things. Journal of Grid Computing, 21(4), 57.

[21] Ali, J., Jhaveri, R. H., Alswailim, M., & Roh, B.-h. (2023). ESCALB: An effective slave controller allocation-based load balancing scheme for multi-domain SDN-enabled-IoT networks. *Journal of King Saud University - Computer and Information Sciences, 35*(6), 101566.

[22] Zeng, Y., & Chu, B. The Appropriate Scale of Competition Between Online Taxis and Taxis Based on the Lotka-Volterra Evolutionary Model. *Journal of Combinatorial Mathematics and Combinatorial Computing, 117*, 25-36.
[23] Yang, Z. (2025). Design of a Visual Communication System for Animated Characters in Virtual Reality Using Sobel Edge Detection and Motion Capture. *Journal of Applied Science and Engineering, 29*(1), 235-243.